Scattered EM-Wave Shaping Using Combination of Cross-Polarization Conversion and Reflection Phase Cancellation

Mustafa K. Taher Al-Nuaimi, Yejun He, *Senior Member, IEEE*, and Wei Hong, *Fellow, IEEE*

***Abstract*—The design of millimeter-wave 1 bit coding engineered reflector for backscattered electromagnetic (EM)-wave shaping by combining both cross-polarization conversion and reflection phase cancellation principles is presented in this letter. The anisotropic unit cell of the presented engineered reflector can efficiently rotate the polarization of an incident EM wave to its orthogonal one at millimeter-wave regime. Each unit cell has four inverted L-shaped copper resonators on the top side of a PEC-backed dielectric substrate. The proposed unit cell has three plasmon resonance frequencies at 87.3, 90.1, and 91.8 GHz with 100% cross-polarization conversion efficiency at these frequencies, and more than 92.1% from about 86.7 to 91.9 GHz. Moreover, if the proposed anisotropic unit cell ("0" element) along with its mirrored one ("1" element) are arranged in one engineered reflector, a 180° ± 25° reflection phase difference is valid between their reflection phases and engineered reflectors that can efficiently manipulate the reflected EM-wave and generates many kinds of scattering patterns such as two lobes, three lobes, four lobes, or even a diffuse scattering pattern can be composed using only those two unit cells. Full-wave simulation, fabrication, and experimental characterization results are presented.**

***Index Terms*—Diffuse reflection, metasurface, reflectarray, reflective surface.**

I. Introduction

POLARIZATION manipulation of electromagnetic (EM) waves and backscattered EM-wave shaping using artificially engineered surfaces has been a topic of interest in the past few years [1]–[14]. Polarization manipulation includes, for instance, linear-to-circular polarization [1] and cross-polarization conversion [2]–[3]. In [2], a ladder-shaped cross-polarization converter was proposed to convert the incident EM waves of linear polarization to their orthogonal component for the 6.9–15.4 GHz band with about 90% polarization conversion efficiency. In [3], a unit cell of intersected square-shape metallic resonators was used to compose the cross-polarization converter surface for the 7.57–20.46 GHz band. Combining polarization rotation and phase cancellation principles for backscattered EM-wave shaping [radar cross section (RCS) modification] is a hot topic recently [4]–[8]. In [4], the monostatic RCS reduction of a slot antenna array was achieved using polarization conversion surface that is composed by a fishbone-like unit cell. In [5], a unit cell that is the combination of cut-wire and oblique split-ring resonator is used to the form a metasurface for cross-polarization conversion and RCS reduction over the frequency band 9.4–19.2 GHz. In [6], RCS reduction of a microstrip antenna was achieved by using polarization rotator surface that is composed by a unit cell consisting of two pairs of L-shape patches.

In a 1-bit coding reflective surface, two unit cells of 0° and 180° reflection phases are required to realize the coding sequence or have a phase difference of about 180° ± 37° between the phases of their reflection coefficients [9], [10]. In [9], a 1 bit coding metasurface was proposed for shaping the backscattered fields and RCS modification for 7.8–12 GHz band by carefully coding ("0" or "1") the unit cells across the 1-bit surface aperture using subwavelength unit cells with the random distribution of unit cells.

In this letter, a simple-structure anisotropic unit cell is proposed and used to form a 1 bit engineered reflective surface that can efficiently rotate the polarization of incident EM-waves to its orthogonal component at millimeter waves (W-band). The unit cell has three resonant frequencies (87.3, 90.1, and 91.8 GHz) with 100% polarization conversion ratio (PCR) at these frequencies and more than 92.1% over the whole frequency band. In addition, based on the phase cancellation technique, the anisotropic unit cell as "0" element and its mirrored one as "1" element are used to design a 1 bit engineered reflector that can efficiently shape the backscattered EM wave and both RCS level and pattern, as will be shown in this letter.

II. Design of the Anisotropic Unit Cell

The anisotropic unit cell (building block) employed in this letter is shown in Fig. 1 and has four inverted L-shaped copper resonators on the upper side of a PEC-backed high-frequency dielectric material ($\varepsilon_r = 10.2$ and $h = 1.27$ mm). To investigate the cross-polarization reflection behavior of this anisotropic

Manuscript received November 7, 2018; revised December 11, 2018; accepted December 23, 2018. Date of publication December 27, 2018; date of current version February 1, 2019. This work was supported in part by the National Natural Science Foundation of China under Grant 61871433 and Grant 61828103; in part by the Shenzhen Science and Technology Programs under Grant GJHZ20180418190529516, Grant JCYJ20170302150411789, Grant JCYJ20170302142515949, and Grant GCZX2017040715180580; and in part by the Guangzhou Science and Technology Program under Grant 201707010490. *(Corresponding author: Yejun He.)*

M. K. T. Al-Nuaimi and Y. He are with the Shenzhen Key Laboratory of Antennas and Propagation, College of Information Engineering, Shenzhen University, Shenzhen 518060, China (e-mail: mustafa.engineer@yahoo.com; heyejun@126.com).

W. Hong is with the State Key Laboratory of Millimeter Waves, School of Information Science and Engineering, Southeast University, Nanjing 210096, China (e-mail: weihong@seu.edu.cn).

Digital Object Identifier 10.1109/LAWP.2018.2889900

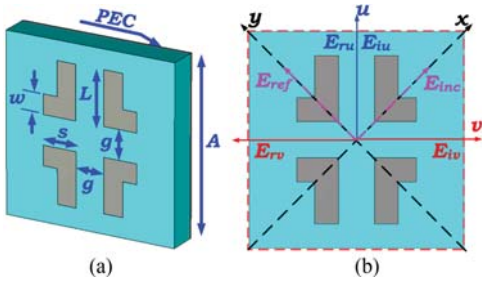

Fig. 1. (a) Geometry of the anisotropic unit cell: $\varepsilon_r = 10.2$, $A = 2$ mm, $L = 0.7$ mm, $s = 0.4$ mm, $g = 0.3$ mm, and $w = 0.2$ mm. (b) Incident and reflected field components.

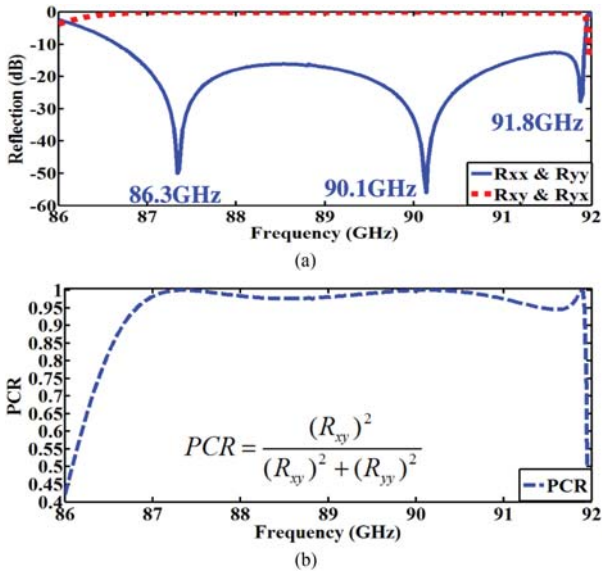

Fig. 2. Reflection characteristics of the anisotropic unit cell. (a) Co-pol and cross-pol reflection coefficients. (b) PCR.

unit cell, Frequency-Solver of the electromagnetic simulation software CST Microwave Studio with appropriate boundary conditions is used. The anisotropic unit cell (placed in the xy plane with its center at the origin) is surrounded by unit-cell boundary conditions in both x- and y-directions and floquet ports in $\pm z$-directions for cross-pol and co-pol reflections (phase and magnitude) extraction. The incident EM wave is assumed to be polarized along x- or y-axis. For the sake of simplicity of the analysis and without loss of generality, a pair of symmetric axes named u-axis and v-axis are introduced with $\pm 45°$ directions with respect to the x-axis. Using the aforementioned simulation setup in CST Microwave Studio and after carrying out a series of numerical simulations, the optimal geometrical dimensions of the anisotropic unit cell are achieved as shown in Fig. 1(a) with the incident and reflected field vectors sketch in Fig. 1(b).

The co-pol and cross-pol reflection coefficients under normally incident linearly polarized plane waves are calculated first, and the results are presented in Fig. 2(a). The co-pol ($R_{\rm xx}$ and $R_{\rm yy}$) and cross-pol ($R_{\rm xy}$ and $R_{\rm yx}$) results presented in Fig. 2(a) show a clear cross-pol conversion over the frequency range from about 86.5 to 91.9 GHz under x-polarized EM waves. To get a deep understanding of the polarization rotation performance of this anisotropic unit cell, the PCR versus frequency is calculated using $R_{\rm xy}$ and $R_{\rm yy}$ components and presented in Fig. 2(b) where the subscripts x and y in the formula in Fig. 2(b) stand for the polarization direction of the incident EM wave. The proposed unit cell shows polarization conversion efficiency of more than 92.1% over the whole frequency band from 86.7 to 91.9 GHz. The anisotropic unit cell has three plasmon resonance frequencies generated by symmetric and antisymmetric couplings of the currents on the L-shaped resonators and ground sheet at 87.3, 90.1, and 91.8 GHz. The plasmon resonance frequencies are determined based on the current distribution by looking at the direction of the induced current flowing [2], [3]. Surface current distribution maps on the L-shaped resonators and ground layer are simulated at resonant frequencies. The results are not presented for brevity.

As can be seen in Fig. 1(b), the incident EM waves along x- or y-axis can be decomposed into two components ($E_{\rm iu}$ and $E_{\rm iv}$) along u-axis and v-axis. The reflection phase versus frequency of the reflected components $E_{\rm ru}$ and $E_{\rm rv}$ are computed, and the simulated results are shown in Fig. 3(a), which shows that the phases [Phase ($E_{\rm ru}$) and Phase ($E_{\rm rv}$)] of those two components are varied from $-180°$ to $+180°$ because of the anisotropy of the unit cell geometry. The reflection phase difference [Phase ($E_{\rm ru}$) – Phase ($E_{\rm rv}$)] of the anisotropic unit cell is computed as shown in Fig. 3(b), and it is about $180° \pm 25°$. The relation between the phase difference and both PCR and RCS reduction are calculated and presented in Fig. 3(c) and (d). As can be seen, to ensure high cross-polarization conversion efficiency of more than 90%, which is required for good EM-wave manipulation [11], and RCS reduction of more than 10 dB [12]–[14], the phase difference should be around $180° \pm 37°$, and the proposed unit cell has a reflection phase difference within this range. In the formula in Fig. 3(d), $\rm Ph_1$ and $\rm Ph_2$ are the reflection phases of the adjacent unit cells, while A_1 and A_2 are their reflection coefficients magnitudes. The complete derivation of the formulas in Fig. 3(c) and (d) can be found in [11]–[14] and are not presented here for brevity. These results show that the proposed unit cell can be used to compose a two-dimensional (2-D) engineered reflector that can efficiently rotate the incident (x-polarized or y-polarized) EM waves into its cross-pol (orthogonal) component with EM-wave shaping.

III. Backscattered EM-Wave Shaping

Recently, designs based on combinations of the principle of polarization conversion and backscattered RCS manipulation have been reported in [9]–[11]. This section investigates the possibility of using the proposed unit cell to design engineered reflectors that can manipulate and shape the backscattered EM-wave and RCS patterns. As shown in Fig. 3, when x- or y-polarized EM waves are incident on the proposed unit cell, there is a clear (and almost stable) reflection phase difference between the reflected EM-wave components $E_{\rm ru}$ and $E_{\rm rv}$, and the phase difference results depicted in Fig. 3(b) show that there is about $180° \pm 25°$ phase difference between the waves of those two directions. Thus, if the proposed anisotropic unit cell ("0" element) along with its mirrored one ("1" element) are arranged in a certain way across the engineered reflector surface as shown in Fig. 6, then because of the $180° \pm 25°$ reflection phase difference (phase cancellation) between $E_{\rm ru}$ and $E_{\rm rv}$ components of the adjacent unit cells, the backscattered EM wave can be shaped or would be canceled out in certain directions.

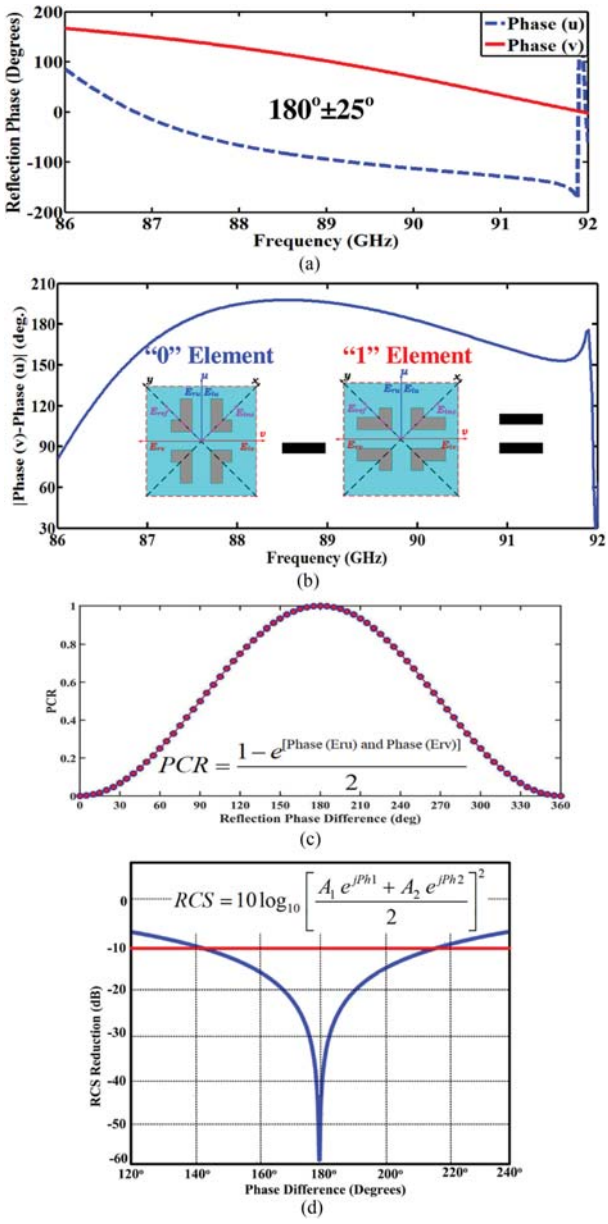

Fig. 3. (a) Reflection phases of an incident wave polarized along u-axis and v-axis. (b) Computed phase difference of the reflected wave (Phase (u) and Phase (v)). (c) PCR. (d) RCS versus reflection phase difference curve.

To validate this hypothesis and to show the ability of the anisotropic unit cell to efficiently manipulate the backscattered patterns, four 1 bit engineered reflective surfaces (named as Surface#1, Surface#2, Surface#3, and Surface#4) with different unit cell distributions are designed as shown in Fig. 4. Each 1 bit surface consists of 8×8 unit cells and occupies an area of 16×16 mm^2, and the "0" and "1" unit cells are distributed according to the distribution map as shown in Fig. 4. Under normal incidence, the backscattered 3-D RCS patterns in Fig. 4 show that the proposed engineered reflectors can strongly manipulate the shape of the backscattered RCS patterns and generate, for instance, two-lobes, three-lobes, four-lobes, or even a diffuse reflection pattern if the anisotropic "0" and "1" cells are distributed in a random order. The diffuse reflection pattern in which the incident EM waves will be reflected with angles other than the

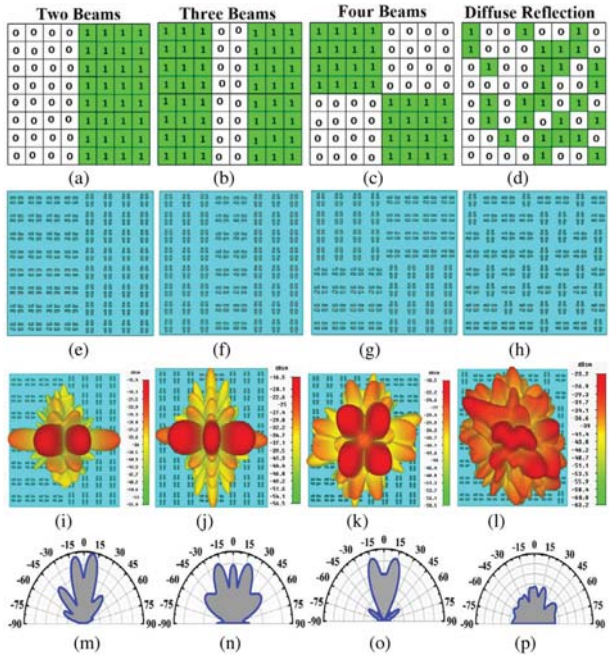

Fig. 4. Layout of the 1 bit engineered reflective surfaces. (a)–(d) Unit cell distribution maps. (e) Surface#1, (f) Surface#2, (g) Surface#3, and (h) Surface#4 are the engineered reflective surfaces. (i)–(l) 3-D backscattered RCS far-field patterns. (m)–(p) Polar RCS far-field patterns.

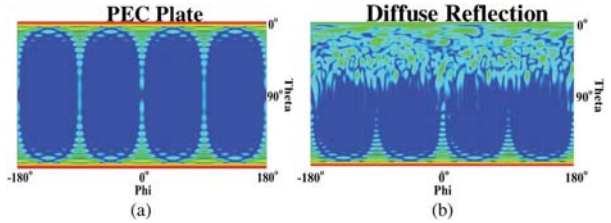

Fig. 5. Two-dimensional field distribution on front of (a) bare PEC plate and (b) Surface#4.

incident angle, in other words, does not obey Snell's law of reflection, which is a very useful radiation pattern for RCS reduction.

It is important here to mention that the shape and level of the backscattered EM-wave and RCS patterns are totally based on the "0" and "1" cells distribution across the engineered reflector aperture. In order to determine the optimum unit cell distribution, various algorithms and programming packages have been used in the literature such as particle swarm optimization in [10], the genetic algorithm in [7] and visual basic in [8], etc. In this letter, a special MATLAB code based on the formulas in [9] is used to determine the optimum unit cell distribution of Surface#4. The 2-D plot of the backscattered EM wave in front of the surface is computed and presented in Fig. 5 along with its equivalent PEC plate for comparison purposes, and a clear diffusion can be noticed in the case of Surface#4. The backscattered RCS patterns of Surface#4 and a metal plate of equal size (16×16 mm^2) are computed and presented in Fig. 6 under the oblique incidence of EM waves when $\theta_{\text{inc}} = 15°$, 30° and 45°, where θ_{inc} is the angle of incidence with respect to the z-axis. As can be seen, the backscattered RCS is highly reduced along the boresight line and the incident power is redistributed on several low-level scattered lobes. More than 6 dB

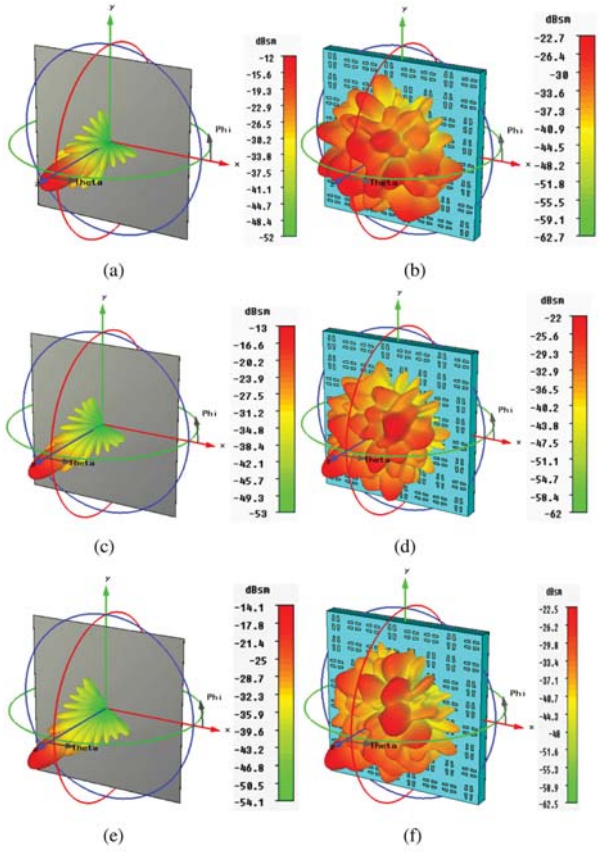

Fig. 6. Three-dimensional RCS far-field patterns of the 1 bit engineered reflector (Surface#4) and bare metal plate under oblique incidence when $\theta_{\rm inc} = 0°$, 15°, 30°, and 45°. (a) PEC plate $\theta_{\rm inc}=15°$. (b) Random surface $\theta_{\rm inc}=15°$. (c) PEC plate $\theta_{\rm inc}=30°$. (d) Random surface $\theta_{\rm inc}=30°$. (e) PEC plate $\theta_{\rm inc}=45°$. (f) Random surface $\theta_{\rm inc}=45°$.

reduction in RCS is achieved over the frequencies 86–92 GHz. In contrast to the case of metal plate under oblique incidence for which the EM wave is reflected according to the classical Snell's law of reflection with angle of incidence always being equal to angle of reflection, Surface#4 efficiently diffuses the incident EM waves, and the backscattered RCS patterns have low-level diffuse pattern compared to a bare PEC case as can be seen in Figs. 4 and 6.

IV. Fabrication and Measurements

To further verify the presented results, a cross-polarization converter surface based on the anisotropic unit cell is fabricated using low-cost printed circuit board technology as shown in Fig. 7(a) and measured inside an anechoic chamber. The dielectric substrate is organic ceramic woven glass from Taconic. The fabricated surface has square aperture, contains 25×25 unit cells, occupies an area of 50×50 mm^2, and follows the same unit cell dimensions presented in Section III. The top layer consists of the anisotropic L-shaped metallic resonators, and the bottom layer is a solid copper sheet. The measurement setup consists of two identical standard-gain W-band horn antennas (to transmit and receive EM waves) connected to the ports of a calibrated network analyzer. Electromagnetic wave absorbers are used to reduce the reflections from surroundings. Furthermore, an

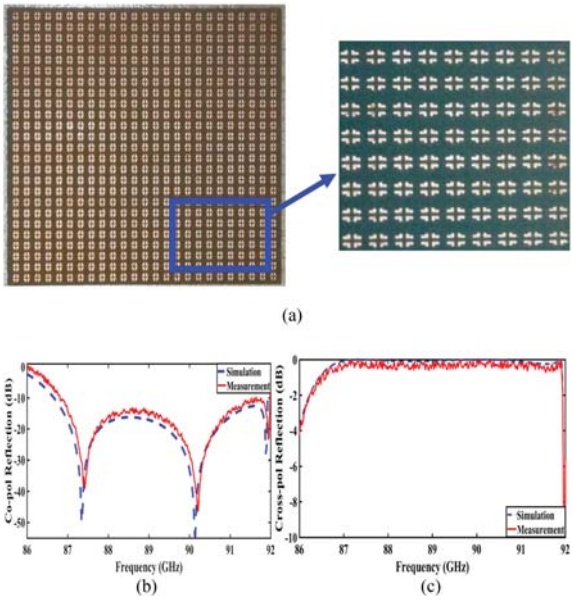

Fig. 7. (a) Fabricated sample. (b) Measured co-pol and (c) cross-pol reflection coefficients.

ultrathin piece of the absorber is installed between the horn antennas to reduce the mutual coupling and to help place the antennas very close to each other during the measurements. Both the surface under test and the horn antennas are placed at the same height and distance between them chosen carefully according to the far-field formula. The measured and simulated co-pol and cross-pol reflection coefficients of the fabricated surface are shown in Fig. 7(c) and (d), which shows that the measured results are a little deviated from the calculated results. This deviation can be attributed to the fabrication error and the misalignment of the horn antennas and the measured surface during the measurements. It is important to mention here that the proposed design is experimentally validated via the measurements of co-pol and cross-pol reflection coefficients, not RCS pattern measurements. This is because of the limitation of the measurement facilities in our anechoic chamber and measurement setup at this frequency band. Furthermore, as can be found in the literature, such kinds of surfaces can be validated via co-pol and cross-pol reflection measurement or RCS pattern measurements or both.

V. Conclusion

One-bit engineered reflectors based on cross-polarization conversion for backscattered EM-wave shaping at millimeter-wave regime are presented in this letter. The anisotropic unit cell composing the surfaces has four-inverted L-shaped copper resonators and three plasmon resonance frequencies at 87.3, 90.1, and 91.8 GHz. The results show that the presented surface can efficiently convert x- or y-polarized incident EM waves to its orthogonal component with about 92.1% polarization conversion efficiency. Moreover, it is shown that the proposed unit cell can be used to design 1 bit engineered reflector for EM-wave shaping and RCS reduction. More than 6 dB of RCS reduction along the boresight axis is achieved when a random unit cell distribution is used.

REFERENCES

[1] H. L. Zhu, S. W. Cheung, K. L. Chung, and T. I. Yuk, "Linear-to-circular polarization conversion using metasurface," *IEEE Trans. Antennas Propag.*, vol. 61, no. 9, pp. 4615–4623, Sep. 2013.

[2] C. Fanga *et al.*, "Design of a wideband reflective linear polarization converter based on the ladder-shaped structure metasurface," *Optik*, vol. 137, pp. 148–155, 2017.

[3] J. Wu, B. Lin, and X. Da, "Ultra-wideband reflective polarization converter based on anisotropic metasurface," *Chin. Phys. B*, vol. 25, no. 8, 2016, Art. no. 088101.

[4] Y. Liu, K. Li, Y. Jia, Y. Hao, S. Gong, and Y. J. Guo, "Wideband RCS reduction of a slot array antenna using polarization conversion metasurfaces," *IEEE Trans. Antennas Propag.*, vol. 64, no. 1, pp. 326–331, Jan. 2016.

[5] W. Jiang, Y. Xue, and S. Gong, "Polarization conversion metasurface for broadband radar cross section reduction," *Prog. Electromagn. Res. Lett.*, vol. 62, pp. 9–15, 2016.

[6] S. Zou, J. Wei and X. Man, "Wideband RCS reduction of patch antenna using PRRS," *Electron. Lett.*, vol. 53, no. 8, pp. 522–524, 2017.

[7] H. Sun *et al.*, "Broadband and broad-angle polarization-independent metasurface for radar cross section reduction," *Sci. Rep.*, vol. 7, 2017, Art. no. 40782.

[8] X. Luo, Q. Zhang, and Y. Zhuang, "Ti-chi-inspired pancharatnam-berry phase metasurface for dual-band RCS reduction," in *Proc. IEEE Int. Symp. Antennas Propag., USNC/URSI Nat. Radio Sci. Meeting*, 2017, pp. 83–84.

[9] T. J. Cui, M. Q. Qi, X. Wan, J. Zhao, and Q. Cheng, "Coding metamaterials, digital metamaterials and programmable metamaterials," *Light, Sci. Appl.*, vol. 3, 2014, Art. no. e218.

[10] L.-H. Gao *et al.*, "Broadband diffusion of terahertz waves by multi-bit coding metasurfaces," *Light, Sci. Appl.*, vol. 4, 2015, Art. no. e324.

[11] Z. Liu, Y. Liu, and S. Gong, "Gain enhanced circularly polarized antenna with RCS reduction based on metasurface," *IEEE Access*, vol. 6, pp. 46856–46862, 2018.

[12] W. Chen, C.A. Balanis, and C. Birtcher, "Checkerboard EBG surfaces for wideband radar cross section reduction," *IEEE Trans. Antennas Propag.*, vol. 63, no. 6, pp. 2636–2645, Jun. 2015.

[13] A. Y. Modi, C. A. Balanis, C. R. Birtcher, and H. Shaman, "Novel design of ultra-broadband radar cross section reduction surfaces using artificial magnetic conductors," *IEEE Trans. Antennas Propag.*, vol. 65, no. 10, pp. 5406–5417, Jul. 2017.

[14] S. H. Esmaeli and S. H. Sedighy, "Wideband radar cross-section reduction by AMC," *Electron. Lett.*, vol. 52, no. 1, pp. 70–71, 2016.